Hindawi Publishing Corporation
Advances in Materials Science and Engineering
Volume 2012, Article ID 985762, 9 pages
doi:10.1155/2012/985762

Research Article

Enhancing the Out-Coupling Efficiency of Organic Light-Emitting Diodes Using Two-Dimensional Periodic Nanostructures

Qingyang Yue, Wei Li, Fanmin Kong, and Kang Li

School of Information Science and Engineering, Shandong University, Jinan 250100, China

Correspondence should be addressed to Kang Li, kangli@sdu.edu.cn

Received 10 March 2012; Revised 17 April 2012; Accepted 19 April 2012

Academic Editor: Jwo-Huei Jou

Copyright © 2012 Qingyang Yue et al. This is an open access article distributed under the Creative Commons Attribution License, which permits unrestricted use, distribution, and reproduction in any medium, provided the original work is properly cited.

The out-coupling efficiency of planar organic light emitting diodes (OLEDs) is only about 20% due to factors, such as, the total internal reflection, surface plasmon coupling, and metal absorption. Two-dimensional periodic nanostructures, such as, photonic crystals (PhCs) and microlenses arrays offer a potential method to improve the out-coupling efficiency of OLEDs. In this work, we employed the finite-difference time-domain (FDTD) method to explore different mechanisms that embedded PhCs and surface PhCs to improve the out-coupling efficiency. The effects of several parameters, including the filling factor, the depth, and the lattice constant were investigated. The result showed that embedded PhCs play a key role in improving the out-coupling efficiency, and an enhancement factor of 240% was obtained in OLEDs with embedded PhCs, while the enhancement factor of OLEDs with surface PhCs was only 120%. Furthermore, the phenomena was analyzed using the mode theory and it demonstrated that the overlap between the mode and PhCs was related to the distribution of vertical mode profiles. The enhancement of the extraction efficiency in excess of 290% was observed for the optimized OLEDs structure with double PhCs. This proposed structure could be a very promising candidate for high extraction efficiency OLEDs.

1. Introduction

Due to the advantages of a wide viewing angle, a low operating voltage, a fast response time, and flexibility, organic light emitting diodes (OLEDs) have rapidly progressed in recent years and have been successfully applied in flat panel displays and solid-state lighting [1–3]. The extraction efficiency η_{ext} is related to the internal quantum efficiency η_{int} of the organic material and the out-coupling efficiency η_{out} of the multilayer planar structure:

$$\eta_{\text{ext}} = \eta_{\text{int}}\eta_{\text{out}}. \tag{1}$$

The intrinsic efficiency has been considerably improved by the use of phosphorescent harvesters [4]. However, the out-coupling efficiency of OLEDs remains very poor (it is only about 20%). This arises from Snell's law. Because of the high refractive index of indium-tin-oxide (ITO)/organic layers and substrate layer, only a small fraction of total light is able to escape from the light-emitting dielectric medium into the air. The photons emitted in the active region of OLEDs are coupled into three types of modes: the mode of direct transmission into the air, the glass total internal reflection mode, and the high index ITO/organic guided mode. There have been various methods to increase the extraction efficiency of OLEDs. These methods can be divided into two categories, one is to place some nanostructures or low index materials on the substrate-air interface for the extraction of substrate-guided modes, such as, substrate surface roughening [5] and use of microlenses arrays [6]. The other is to insert some periodic nanostructures between the metallic cathode and the substrate layer to recover the waveguide loss in the ITO/organic layer, for example, using a refractive index modulation layer [7] or photonic band gap structure [8].

Two-dimensional periodic nanostructures (photonic crystals, PhCs) have previously been used with the aim of increasing the extraction efficiency of GaN-based light-emitting diodes (LEDs) [9, 10]. Similarly, PhCs structure can be added to OLEDs devices to increase the out-coupling efficiency. OLED out-coupling efficiency levels can be improved by optimizing the structural characteristics of the 2D PhCs, particularly the lattice constant (the period), the depth, the filling factor, and the lattice symmetry (square or triangle lattice).

This paper is organized as follows. In the second section, we provide a structural model of actual OLEDs in order to analyze the mechanisms that affect the light out-coupling characteristics. In this part, the mechanisms by which the 2D PhCs structures enhance the out-coupling efficiency of OLEDs are also given. In Section 3, we employ the finite-difference time-domain (FDTD) method to simulate the out-coupling efficiency of the OLEDs and describe the architecture of the device used in simulations. In Section 4, in order to find the optimal structure, we scan the structural characteristics of 2D periodic nanostructures (embedded PhCs and surface PhCs), such as, the period, the depth, and the filling factor. The influence of 2D periodic nanostructures on enhancing the out-coupling efficiency of the OLEDs is discussed, and then it is found the embedded PhCs have a key action in improving the out-coupling efficiency (about 240%) but the contribution of the surface PhCs is poor (only about 120%). Furthermore, we analyze the phenomena using the mode theory, and it demonstrates that the overlap between the mode and PhCs is related to the vertical mode profiles. At the end of this part, an optimized OLEDs structure with surface PhCs on the top of the substrate and embedded PhCs between the ITO layer and the substrate layer is designed. Finally, the conclusion is presented.

2. The OLEDs Microcavity Model and the PhCs

A schematic diagram of the OLEDs structure is shown in Figure 1. The typical OLEDs structure is a multilayer planar structure with the reflective metal contact layer, the ITO layer ($n = 1.8 \sim 2.0$), the substrate layer ($n = 1.5$), and the organic layer ($n \approx 1.8$) which includes a hole injection layer, a hole transporting layer, an emitting layer, an electron transporting layer, and an electron injection layer. A small fraction of the emitted light is directed into the air because the total internal reflection can occur at the glass-ITO interface and the air-glass interface. This leads to the conception of Fabry-Perot (F-P) microcavity OLEDs [11]. The out-coupling losses are caused by the surface plasmon polaritons (SPPs), the waveguide mode, the substrate mode, and the electrode absorption, as shown in Figure 1. Due to the SPPs at the interface of the metal and the organic (dielectric), about 36% of the generated light is dissipated as scattered light or as nonradiative emission in the cathode region. According to the total internal reflection that occurs at the glass-ITO interface and the air-glass interface, a greater portion of the emitted light is confined within the substrate layer and organic/ITO layer that can be guided as the substrate mode (22%) and the waveguide mode (20%). Four percent of generated light is absorbed by the metal electrodes. Thus, only about 18% of the light can escape from planner OLEDs. The total energy that is trapped as the substrate mode and the waveguide mode is up to 40%. In order to improve the light extraction efficiency, first the light that is confined within the substrate layer and the organic/ITO layer from the conventional planar structure of OLEDs should be extracted.

PhCs have previously been used to improve the extraction efficiency of GaN-based LED, and the best light extraction efficiency of the PhCs LED achieves 73% without using encapsulants [12]. PhCs are dielectric perturbations on the scale of the wavelength, offering control of the way light propagates in the medium. A guided mode that propagates within the high index layer can be characterized by an efficient index n_{eff}, smaller than the substrate index n_{sub}, whose wavevector is

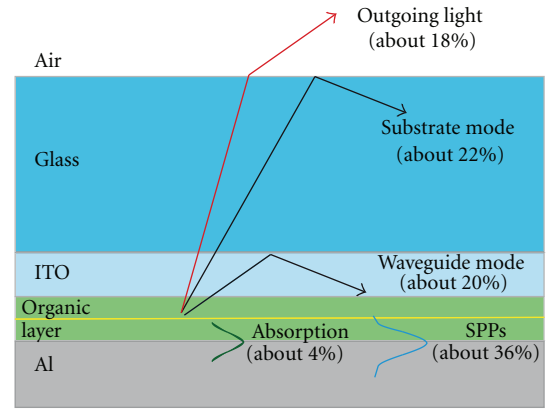

Figure 1: Kinds of light out-coupling losses in ordinary OLEDs.

$$k_{//} = \frac{n_{\text{eff}}\,\omega}{c} = \frac{n_{\text{sub}}\sin(\theta_m)\omega}{c},$$
$$\theta_m \geq \theta_c = \arcsin\left(\frac{n_{\text{low}}}{n_{\text{sub}}}\right), \tag{2}$$

where n_{low} is the index of the low index layer, θ_m is the mode propagation angle, and θ_c is the angle of total reflection. If the mode wavevector is $k_{//} = n_{\text{eff}}\omega/c \leq n_{\text{low}}\omega/c$, the light will radiate from the substrate layer into the low index layer and form the leaky mode. In the presence of PhCs, the guided modes become Bloch modes [12] and the wavevector $k_{//}$ is now coupled to other harmonics $k_{//} + G$ by the reciprocal lattice vectors G, increasing extraction efficiency. To diffract the guided light into the low index layer, the lattice constant p of the PhCs needs to satisfy the diffraction condition,

$$k_{//} = |k_{//} + mG_0| \leq \frac{n_{\text{low}}\,\omega}{c}, \tag{3}$$

where $G_0 = 2\pi/p$ and m is an integer (determining which harmonic is responsible for diffraction to the low refractive index layer). The Bloch mode is then referred to as a leaky mode, because its power leaks to the low index layer as it propagates. So the PhCs can improve the light extraction efficiency of the OLEDs. The diffraction condition depends on the wavelength, the lattice constant, and the mode propagation angle.

3. Numerical Analysis

In this study, the three-dimensional (3D) FDTD method was employed for simulations, which is a space and time discretization of Maxwell curl equations [13]. The FDTD calculation domain is shown in Figure 2. The simulation structure was composed of a glass layer, a SiN_x layer, an ITO layer, an organic layer, and a metal contact layer. The 2D PhCs were

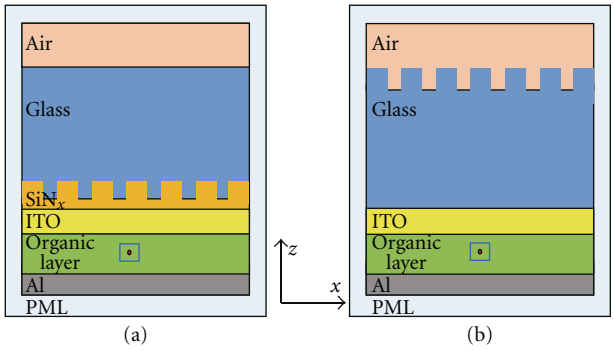

Figure 2: Schematics of OLED structure with (a) embedded PhCs between the ITO layer and the substrate (b) surface PhCs etched on the substrate.

embedded in a glass-substrate interface or located on the top surface of the glass layer, as shown in Figures 2(a) and 2(b). Dipole sources were chosen as the excitation source since it has been proved that the electron-hole-recombination can classically be represented by a dipole [14]. Multiple dipole sources are intrinsically suited for the simulation of the active layer in 3D FDTD method. Nevertheless, the attempt of using multiple dipole sources as well as periodic continuation boundary conditions is not convenient since it will lead to a nonphysical interference pattern. Therefore, a single dipole source within a finite computational domain was chosen. Furthermore, a perfectly matched layer (PML) [15] enclosing the entire simulation domain was used to absorb outgoing waves and avoid nonphysical reflections (see Figure 2). In addition, inhomogeneous mesh was used during the simulation, the grid size was 15 nm in the x and y directions and 10 nm in the z direction.

The power loss in materials (ITO and glass) during the simulation was ignored since the imaginary part of the ITO and glass index is closed to zero at the wavelength of 0.55 μm (see Figure 3) [16].

The extraction efficiency η_{ext} was calculated from the power flux extracted from the OLEDs P_{out} with respect to the overall emitted power from the active layer P_{emit} (see Figure 2):

$$\eta_{\text{ext}} = \frac{P_{\text{out}}}{P_{\text{emit}}} = \frac{P^{+}_{z,\text{out}}}{P^{+}_{x,\text{in}} + P^{-}_{x,\text{in}} + P^{+}_{y,\text{in}} + P^{-}_{y,\text{in}} + P^{+}_{z,\text{in}} + P^{-}_{z,\text{in}}}. \tag{4}$$

With $P^{+}_{z,\text{out}}$ the power flow integrated over a plane just above the OLEDs structure and $P_{x,y,z,\text{in}}$ the integrated power flux through the planes normal to x, y, or z enclosing the source. The + and − signs indicate power flow parallel or antiparallel to the corresponding axis.

The extraction efficiency enhancement factor F is defined as follow:

$$F = \frac{\eta_{\text{ext}}}{\eta_{\text{con}}}, \tag{5}$$

where η_{ext} is the extraction efficiency of the OLEDs with PhCs structures, and η_{con} is the extraction efficiency of the conventional OLEDs.

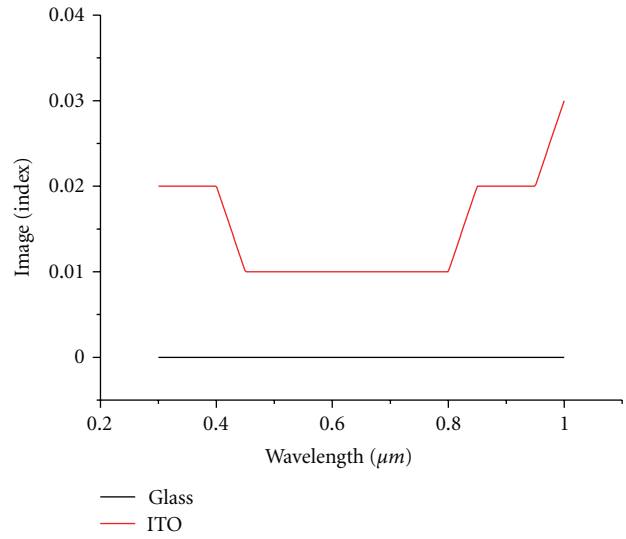

Figure 3: The imaginary part of the index as a function of wavelength. The solid red line shows the imaginary part of the index of ITO while the solid black line shows the imaginary part of the index of glass.

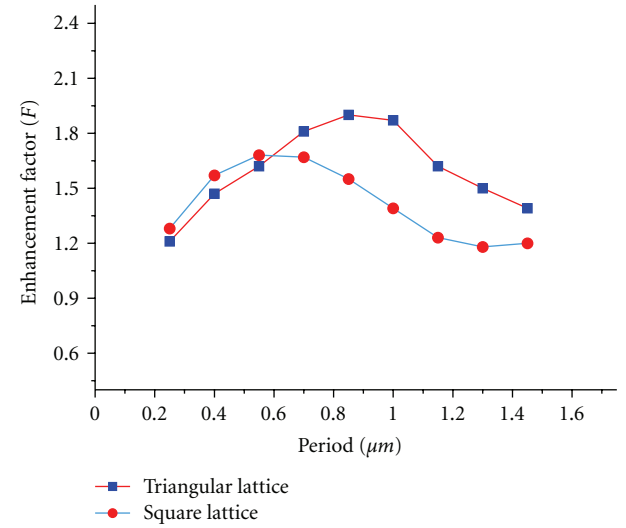

Figure 4: The enhancement factor of triangular lattice PhCs and square lattice PhCs as a function of period.

In the following, the continued guided wave was used as the source in the organic layer, with its vacuum wavelength of 0.55 μm at the plane in the center of the organic layer. The enhancement of the output coupling efficiency was studied based on the standard embedded PhCs with the filling factor $f = 0.35$ and the etched depth $d = 0.3\,\mu$m (as shown in Figure 2(a)), when the period varied from 0.3 μm to 1.4 μm (see Figure 4). The filling factors of triangular lattice and square lattice PhCs are expressed, respectively, as follows [17]

$$f_{\text{triangular}} = \frac{2\pi R^2}{\sqrt{3}p^2}, \qquad f_{\text{square}} = \frac{\pi R^2}{p^2}, \tag{6}$$

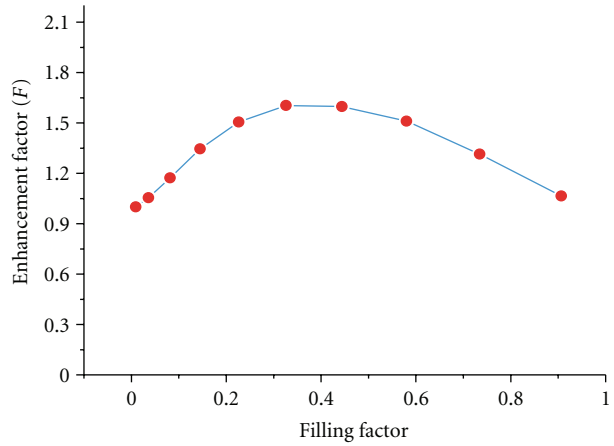

Figure 5: Enhancement of the out-coupling efficiency as a function of filling factor.

where, R is the radius of the hole which is filled with the glass in Figure 2(a) or air hole in Figure 2(b). From Figure 4, it can be seen that the enhancement factor of triangular PhCs was approximately equal to the square lattice PhCs when the period was changed from 0.3 μm to 0.7 μm. However, the F of triangular PhCs was obviously much larger than the square lattice with the period was between 0.7 μm to 1.4 μm. And the average F of triangular lattice was also larger than the square lattice PhCs. Thus, triangular lattice PhCs were selected for the next simulations, since they have better performances than square ones.

The dependence of the enhancement factor F on the PhCs filling factor is illustrated in Figure 5 which shows that the F is lower when the filling factor is too small or too large. The highest enhancement was obtained at about $f = 0.4$. These results are in agreement with [18].

Optimization of the PhCs is difficult, because it involves solving a multiparameter inverse problem. There are countless combinations of vacuum wavelength, lattice symmetry, period (lattice constant), filling factor and depth of PhCs, and it is impossible to say which one gives the most efficient PhCs structure in releasing the trapped energy in the OLEDs structure. From the above discussion, in order to simplify the problem we choose triangular lattice PhCs with filling factor $f = 0.35$ to analyze the enhancement of the out-coupling efficiency using the vacuum wavelength $\lambda = 0.55\,\mu$m. In the next section, we concentrate on studying the influence of the PhCs parameters, such as, lattice constant (period), depth of the PhCs and thickness of the ITO layer on the enhancement of the output-coupling efficiency.

4. Simulation Results and Discussion

4.1. Influence of the Embedded PhCs on the Enhancement of the Out-Coupling Efficiency. For an OLED with embedded PhCs, the dependence of the enhancement on the PhCs parameters was calculated based on a standard embedded PhCs structure with the period $p = 0.5\,\mu$m, the depth $d = 0.3\,\mu$m, the thickness of the SiN_x layer $T = 0.4\,\mu$m, and the height of the ITO layer $h = 0.2\,\mu$m as shown in Figure 2(a). Each parameter was varied in turn while other parameters were kept constant, and the enhancement factor F was calculated. Different Fs of light out-coupling efficiency with period p varying from 0.3 μm to 1.4 μm were calculated as illustrated in Figure 6(a). From Figure 6(a), it can be seen that F was low when the p was too small or too large. The F was kept at a larger value when the p was changed from 0.5 μm to 1.1 μm. The wavevector $k_{//}$ became Bloch mode and radiated from the substrate layer into the low index layer by the reciprocal lattice vectors G according to the theory in Section 2. The reciprocal lattice vectors G was decided on by the period p of the PhCs. Evidently, each guided mode has a separate optimum reciprocal lattice vector for maximum extraction and is diffracted into the lower refractive index layer. The OLEDs structure is a multimode waveguide, and the single period hardly enhances the total extraction efficiency of all the modes. Thus, it is reasonable that the p of 0.5 μm $\sim$ 1.1 μm was chosen in the experiment.

The enhancement factor F was plotted as a function of depth in Figure 6(b), which shows that F increased with the depth d increasing. A maximum value of 172% was obtained at a depth of 0.4 μm. In this case, the depth of the PhCs d is equal to the SiN_x layer. It means that a larger F can be obtained by etching PhCs deeply through the SiN_x layer. The F grows as the depth of PhCs increases, and this is related to the overlap of the vertical guided mode profile with the PhCs layer. For small PhCs depth $d < 0.1\,\mu$m, the attenuation length [18] of the guided mode profile within the PhCs layer is larger than the etch depth, hence, a steep increase is found until the mode profile negligibly penetrates into the low index layer. For $d > 0.2\,\mu$m, the enhancement factor grows since the guided mode is squeezed more and more between the metal layer and the PhCs layer.

The effect of the height of the ITO layer h was also investigated. The relationship between enhancement factor F and h which was changed from 0 μm to 0.4 μm is shown in Figure 6(c). The F almost linearly decreased with increasing h, and the largest value 187% was obtained when the height ITO layer was 0 μm. Because the power of the waveguide mode was mostly confined in the region between the ITO/organic layer and the PhCs, the smaller h resulted in high energy concentrated in the PhCs layer. Theoretically, to get the largest enhancement factor, the height of the ITO layer should be chosen as 0 μm. However, this is not reasonable because the ITO layer is the electrode of OLEDs. The PhCs can be directly patterned in the ITO layer of the glass cylinder to replace the PhCs in the SiN_x layer. In addition, there was no noticeable degradation of electrical characteristics under typical operating conditions [19].

The patterned PhCs ITO layer is a good choice to improve the enhancement factor of the out-coupling efficiency. The patterned ITO layer was fabricated by the bellow method, the ITO layer was deeply etched through the organic layer and the holes were filled with glass. The influence of the height of the ITO PhCs H on enhancing the out-coupling efficiency was studied, and the enhancement factor F of out-coupling efficiency was found when H varied from 0 μm to

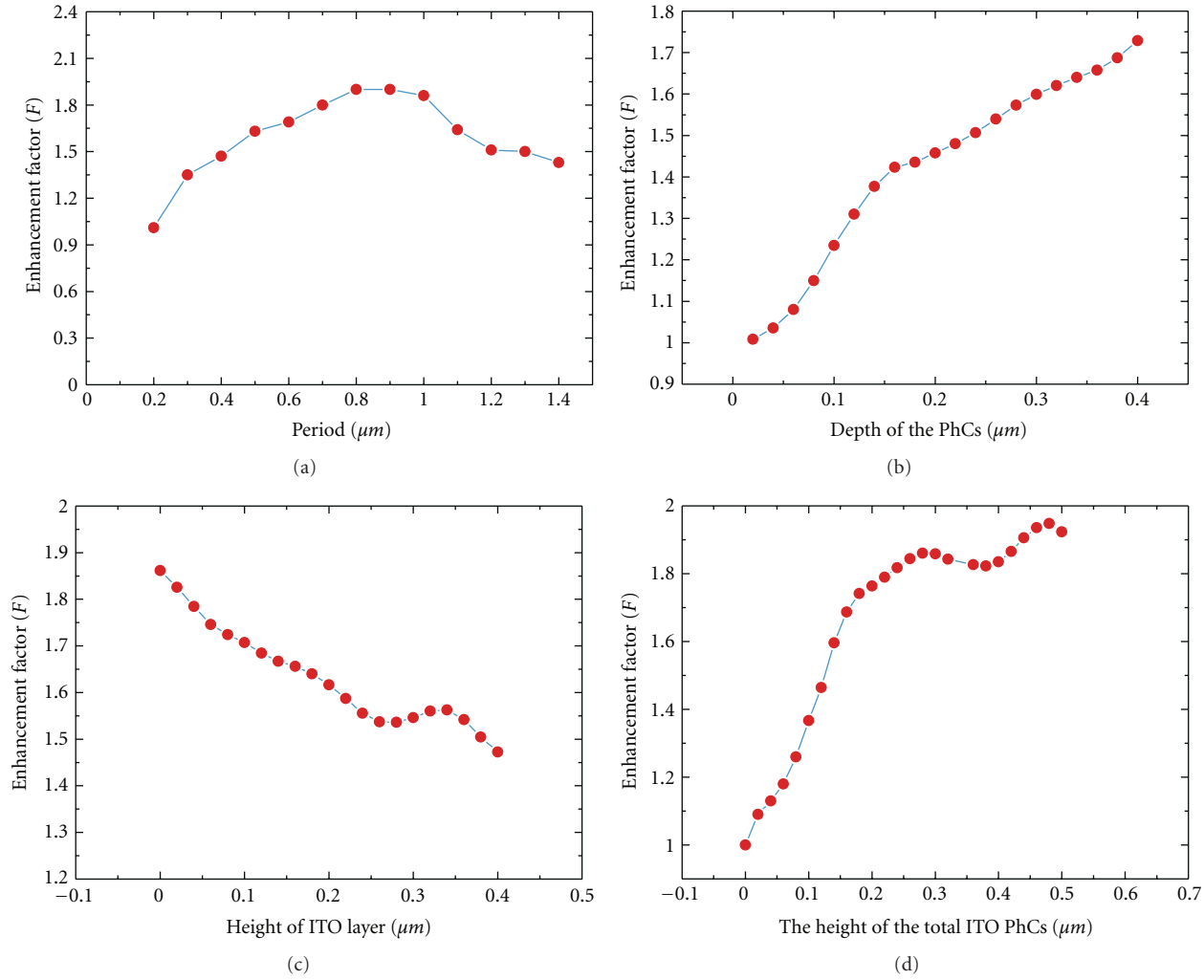

FIGURE 6: Enhancement of light out-coupling efficiency as a function of (a) period of the PhCs p, (b) depth of PhCs embedded in the SiN_x layer d, (c) height of ITO layer h, and (d) height of the total ITO layer H.

0.5 μm in Figure 6(d). The F significantly increased as H was changed from 0 μm to 0.3 μm. The attenuation length [18] of the guided mode profile within the PhCs layer was large than H, and hence a steep increase was found until $H = 0.3\,\mu$m. Then an oscillation could be found in the range of $0.3\,\mu\text{m} < H < 0.5\,\mu$m, and F gradually reached a constant 180%. Since low-order modes are strongly evanescent in the etched region, their diffraction does not significantly increase for H larger than $\sim\lambda/n_{\text{PhC}}$ [9], where n_{PhC} is the average index of the PhCs layer. It can be expressed as follows:

$$n_{\text{PhC}} \approx \sqrt{f\varepsilon_{\text{glass}} + (1-f)\varepsilon_{\text{ITO}}}. \quad (7)$$

The peak occurred at a height H equal to 0.3 μm. However, this ascending trend approximately kept constant at this depth and changed to fluctuation as the PhCs were etched deeper. This implies that there is no additional benefit from a much deeper ITO layer.

To fully explain the variation trend shown in Figure 6(d), the vertical mode profiles of the ordinary OLEDs structures are first discussed as shown in Figure 7 (actually, there are many modes in the multilayer planar structure, we used four modes of these to express the modes profiles). As shown in Figure 7(a), the power of these low order modes was confined in the ITO/organic layer, so the embedded PhCs could be used to improve the out-coupling efficiency by extracting the power of these low order modes. Figure 7(b) is the high-order modes profiles whose power was located

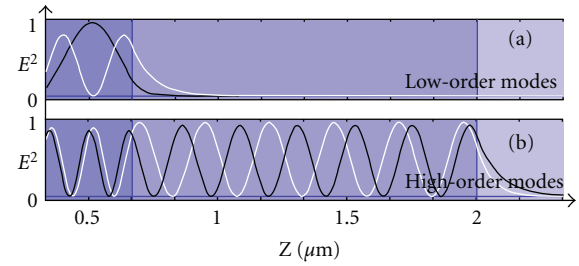

FIGURE 7: The vertical mode profiles of the ordinary OLEDs structures. (a) low-order modes (b) high-order modes.

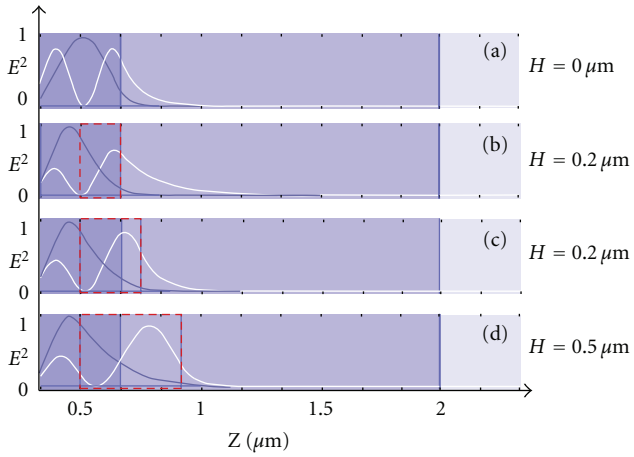

Figure 8: The vertical low-order modes profiles of the OLEDs structure with embedded ITO PhCs. The region in the red rectangle is the PhCs layer.

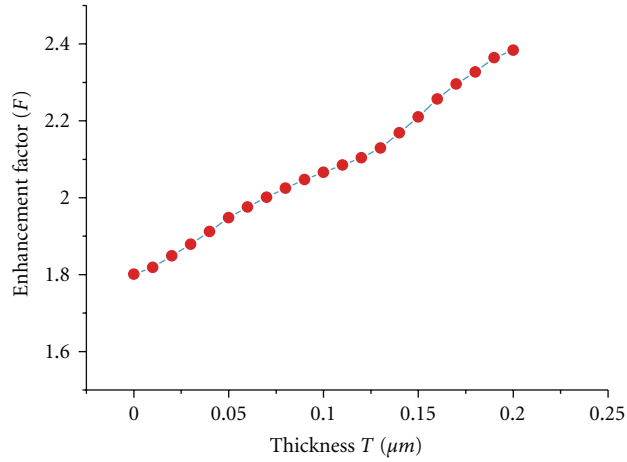

Figure 9: The enhancement factors F of the structure with thickness T.

in the substrate layer. Similarly, the out-coupling efficiency was enhanced using surface PhCs to extract the high-order modes power. Distributions of these low-order modes with ITO PhCs thicknesses H are provided in Figure 8. The index of the PhCs layer can be obtained by the formula (7), which is larger than the index of the glass and smaller than the index of the organic layer. Since, these low modes slowly penetrated into the PhCs layer with H increasing from 0 μm to 0.5 μm, the interaction between the PhCs and these modes increased, and thus the out-coupling efficiency grew with changes in H. When $H = 0.2\,\mu$m, the peak of first-order mode entered into the PhCs layer, and most of the power of the first-order mode escaped from the organic layer. The peak of the ground state mode was out of the PhCs layer, whose power was partly still in the organic layer. The peak of the ground state mode became closer and closer to the PhCs layer with H increasing, and thus the overlap of this mode with the PhCs increased and the power strongly diffracted to the substrate. When $H = 0.5\,\mu$m, the peak of the ground state mode got very close to the PhCs but was still in the high index layer, the out-coupling efficiency kept constant at 180% with a small oscillation.

To get much higher light extraction efficiency, PhCs etched through the active layer have been used in the GaN-based LED [20]. A standard embedded PhCs OLEDs structure with 0.3 μm PhCs pattern ITO layer was used in simulations, and the glass cylinder penetrates into the organic layer with the thickness T. The enhancement factor F of the structure with T varying from 0 μm to 0.2 μm at an interval of 0.01 μm was calculated. These results are shown in Figure 9. It was found that the enhancement factors F almost linearly increased from approximately 180% to 240% when T was changed from 0 μm to 0.2 μm. The turning point occurred at a thickness equal to 0.13 μm. When $T \geq 0.13\,\mu$m, the slope of the increasing line was larger than that for $T \leq 0.13\,\mu$m, and a maximum of 240% was obtained at $T = 0.2\,\mu$m. Similarly, the vertical mode profiles of the ordinary OLEDs structure were studied. As shown in Figure 10, the

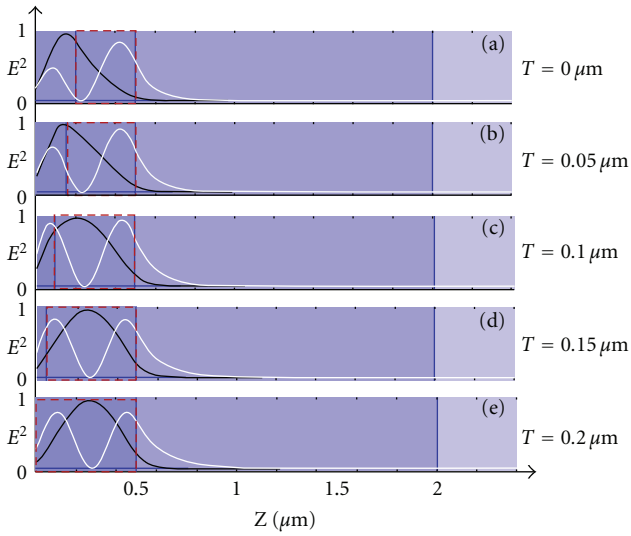

Figure 10: The vertical low-order modes profiles of the OLEDs structure with PhCs embedded into organic layer. The region in the red rectangle is the PhCs layer.

peak of the first-order mode penetrates completely into the PhCs layer, which hardly affects the out-coupling efficiency. To simplify the problem, only the ground state mode is considered. The peak of this mode got closer and closer to the PhCs layer when T was changed from 0 μm to 0.1 μm. This implies that the interaction between the mode and the PhCs becomes stronger and stronger. When $T \geq 0.1\,\mu$m, the peak of ground state mode completely enters into the PhCs layer, the overlap of the mode and PhCs had a much steeper enhancement, and a maximum of 240% was obtained at $T = 0.2\,\mu$m.

4.2. Influence of the Surface PhCs on the Enhancement of the Out-Coupling Efficiency. To analyze the effect of the surface PhCs on the enhancement of the light extraction, we used

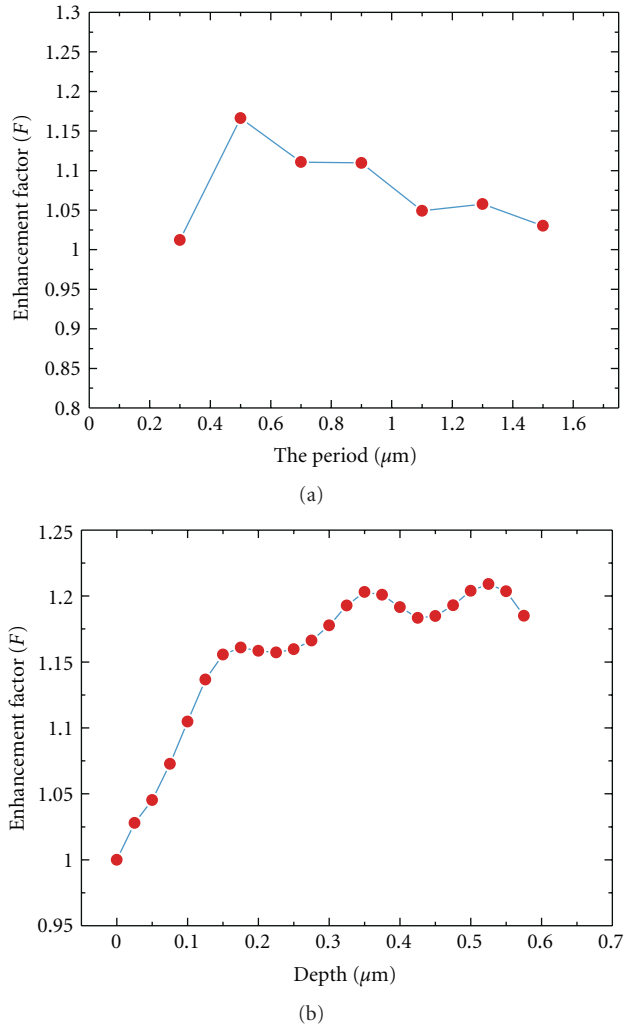

Figure 11: Enhancement of the out-coupling efficiency as a function (a) the period and (b) the depth of PhCs.

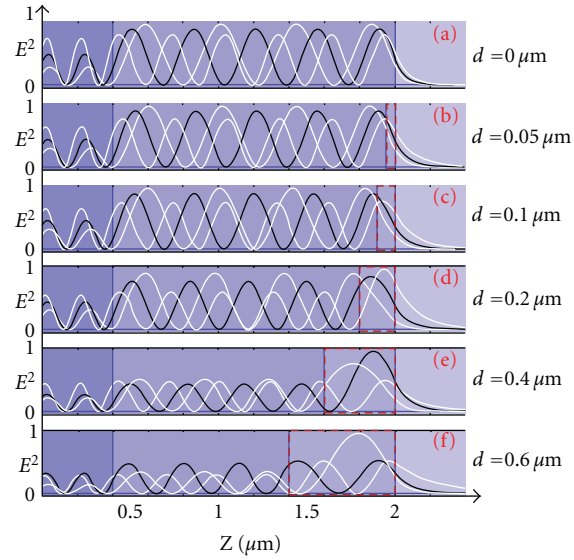

Figure 12: The vertical high-order modes profiles of the OLEDs structure with surface PhCs. The region in the red rectangle is the PhCs layer.

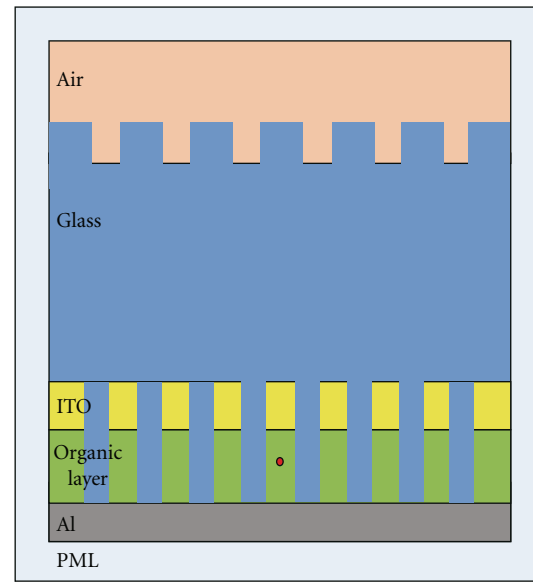

Figure 13: Schematics of optimized OLED structure with embedded PhCs and surface PhCs.

an approach similar to that of the embedded PhCs. We used the surface PhCs structure with the period $p = 0.5\,\mu$m, depth of the PhCs $d = 0.2\,\mu$m as the standard structure (see Figure 2(b)). The enhancement is depicted as a function of the period p and depth d in Figures 10(a) and 10(b). The highest enhancement factor F was obtained at the period of $0.5 \sim 0.9\,\mu$m. The result is close to the embedded PhCs, but somewhat differently, the maximum is only about 120%. From Figure 11(b), it can be found that the light out-coupling efficiency dramatically increased when the surface PhCs were etched from $0\,\mu$m to $0.35\,\mu$m. This is attributed to the strong overlap between the high-order guided modes and PhCs. As shown in Figure 12, the peaks of these modes slowly entered into the PhCs layer with d increasing. Much more power of the high-order guided modes can escape from the substrate layer. When $d \geq 0.35\,\mu$m, this ascending trend stopped and changed to fluctuation as the PhCs were etched deeper. Because peaks of these high-order modes have been located in the PhCs regions, deeper etched PhCs cannot enhance the interaction between these modes and PhCs. This implies that there is no additional benefit from drilling the holes deeper and deeper. From the simulation results, it was found that the surface PhCs play a poor role in enhancing the out-coupling efficiency of the OLEDs (about 120%). In the experiment, the enhancement factor F of about 130% with surface PhCs was obtained [21].

4.3. Optimized OLEDs Structure with Embedded PhCs and Surface PhCs. We designed an OLED structure with embedded PhCs and surface PhCs (see Figure 13). The parameters of embedded PhCs were set as period $p = 0.7\,\mu$m, height

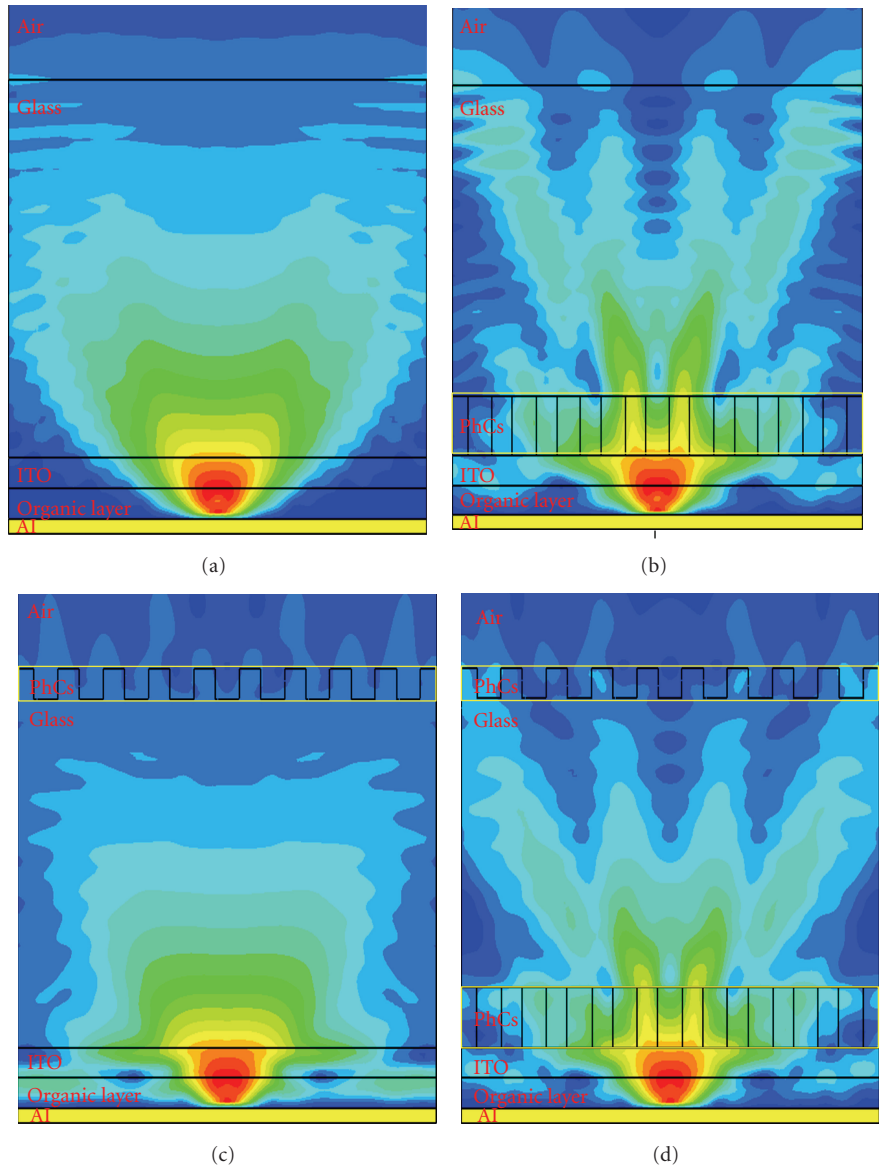

Figure 14: The vertical power distribution of (a) ordinary OLEDs, (b) OLEDs with embedded PhCs, (c) OLEDs with surface PhCs, and (d) OLEDs with embedded PhCs and surface PhCs. The region in the yellow rectangle is the PhCs layer.

of the ITO layer $h = 0.3\,\mu$m, and depth $d = 0.5\,\mu$m. The ITO layer and the organic layer were patterned with PhCs using glass. At the same time, the surface PhCs structure with the period $p = 0.5\,\mu$m and depth $d = 0.3\,\mu$m was etched in the surface of the substrate. An enhancement factor F of 290% was obtained via FDTD simulation. Figure 14(a) shows that with the vertical power distribution of ordinary OLEDs, most of emitted light from the organic layer is confined in the high index layers. The emitted light was redistributed by the embedded PhCs [22] in this structure, as shown in Figure 14(b), since the light can be easily extracted by the embedded PhCs. From the results presented in the Section 4.2, it was found that the top PhCs contribute little to enhance the out-coupling efficiency of OLEDs. The surface PhCs can extract a small fraction of the light (the power of the high order modes), as illustrated in Figure 14(c). The structures with embedded PhCs and surface PhCs (see Figure 14(d)) present an effective way to avoid energy spreading into the ITO/organic layer and substrate layer and contribute to the extraction of low-order modes and high-order modes. This proposed structure could be a very promising candidate for high extraction efficiency OLEDs.

5. Conclusion

In this paper, we employed the finite-difference time-domain (FDTD) method to study the improvement of the out-coupling efficiency using embedded PhCs and surface PhCs. Some parameters of the PhCs including the filling factor, the depth, and the lattice constant were investigated. The

result shows that the embedded PhCs play a key role in enhancing the out-coupling efficiency, a maximum of 187% was obtained using SiN_x PhCs, and the largest value of 240% was obtained when the PhCs were etch into the organic layer. The out-coupling efficiency of the surface PhCs is only about 120%, so it has a poor role in improving the out-coupling efficiency. And then we analyzed the phenomena by using the mode theory, which showed that the low-order modes and high-order modes should be modified to escape from OLEDs using the double PhCs. It demonstrated that the overlap between the mode and PhCs is related to the vertical mode profiles and that it is an effective attempt to enhance the light extraction efficiency by changing the distributions of vertical mode profiles. Finally, the enhancement of the extraction efficiency in excess of 290% was observed for the optimized double photonic crystal pattern. This proposed that structure could be a very promising candidate for high extraction efficiency OLEDs.

Acknowledgments

The work was supported by the National Natural Science Foundation of China (61077043), the National Basic Research Program of China through Grands no. 2009CB-930503 and 2009CB930501. The authors would like to thank Dr. Manfred Hammer of the University of Twente for the codes he provided, which were the basis of mode analyses shown in Figures 8, 9, 11, and 12. The authors would also like to thank Dr. Edward C. Mignot, Shandong University, for linguistic advice.

References

[1] T. Sekitani, H. Nakajima, H. Maeda et al., "Stretchable active-matrix organic light-emitting diode display using printable elastic conductors," *Nature Materials*, vol. 8, no. 6, pp. 494–499, 2009.

[2] E. C. W. Ou, L. Hu, G. C. R. Raymond et al., "Surface-modified nanotube anodes for high performance organic light-emitting diode," *ACS Nano*, vol. 3, no. 8, pp. 2258–2264, 2009.

[3] Z. Yu, L. Hu, Z. Liu et al., "Fully bendable polymer light emitting devices with carbon nanotubes as cathode and anode," *Applied Physics Letters*, vol. 95, no. 20, Article ID 203304, pp. 3304–3307, 2009.

[4] M. A. Baldo, D. F. O'Brien, Y. You et al., "Highly efficient phosphorescent emission from organic electroluminescent devices," *Nature*, vol. 395, no. 6698, pp. 151–154, 1998.

[5] J. Zhou, N. Ai, L. Wang et al., "Roughening the white OLED substrate's surface through sandblasting to improve the external quantum efficiency," *Organic Electronics*, vol. 12, no. 4, pp. 648–653, 2011.

[6] J. H. Lee, Y. H. Ho, K. Y. Chen et al., "Efficiency improvement and image quality of organic light-emitting display by attaching cylindrical microlens arrays," *Optics Express*, vol. 16, no. 26, pp. 21184–21190, 2008.

[7] K. Hong, H. K. Yu, I. Lee, K. Kim, S. Kim, and J. L. Lee, "Enhanced light out-coupling of organic light-emitting diodes: Spontaneously formed nanofacet-structured MgO as a refractive index modulation layer," *Advanced Materials*, vol. 22, no. 43, pp. 4890–4894, 2010.

[8] Y. J. Lee, S. H. Kim, J. Huh et al., "A high-extraction-efficiency nanopatterned organic light-emitting diode," *Applied Physics Letters*, vol. 82, no. 21, pp. 3779–3781, 2003.

[9] A. David, T. Fujii, R. Sharma et al., "Photonic-crystal GaN light-emitting diodes with tailored guided modes distribution," *Applied Physics Letters*, vol. 88, no. 6, 2006.

[10] D. H. Long, I. K. Hwang, and S. W. Ryu, "Design optimization of photonic crystal structure for improved light extractionof GaN LED," *IEEE Journal on Selected Topics in Quantum Electronics*, vol. 15, no. 4, pp. 1257–1263, 2009.

[11] H. Benisty, H. De Neve, and C. Weisbuch, "Impact of planar microcavity effects on light extraction—Part I: basic concepts and analytical trends," *IEEE Journal of Quantum Electronics*, vol. 34, no. 9, pp. 1612–1631, 1998.

[12] J. J. Wierer, A. David, and M. M. Megens, "III-nitride photonic-crystal light-emitting diodes with high extraction efficiency," *Nature Photonics*, vol. 3, no. 3, pp. 163–169, 2009.

[13] A. Taflove and S. C. Hagness, *Computational Electrodynamics: The Finite-Difference Time-Domain Method*, Artech House, Norwood, Mass, USA, 2005.

[14] H. Benisty, R. Stanley, and M. Mayer, "Method of source terms for dipole emission modification in modes of arbitrary planar structures," *Journal of the Optical Society of America A*, vol. 15, no. 5, pp. 1192–1201, 1998.

[15] J. P. Berenger, "A perfectly matched layer for the absorption of electromagnetic waves," *Journal of Computational Physics*, vol. 114, no. 2, pp. 185–200, 1994.

[16] P. Vandersteegen, C. Van Buggenhout, P. Bienstman, and R. Baets, "Numerical investigation of a 2D-grating for light extraction of a bottom emitting OLED," in *Proceedings of the International Conference on Transparent Optical Networks (ICTON '06)*, vol. 2, pp. 211–214, June 2006.

[17] A. David, *High-efficiency GaN-based light-emitting diodes: light extraction by photonic crystals and microcavities*, Ph.D. thesis, Ecole Polytechnique, Palaiseau, France, 2006.

[18] C. Wiesmann, *Nano-structured LEDs-Light extraction mechanisms and applications*, Ph.D. thesis, Science Faculty, Universität Regensburg, Regensburg, Germany, 2009.

[19] Y. R. Do, Y. C. Kim, Y. W. Song, and Y. H. Lee, "Enhanced light extraction efficiency from organic light emitting diodes by insertion of a two-dimensional photonic crystal structure," *Journal of Applied Physics*, vol. 96, no. 12, article 8, pp. 7629–7636, 2004.

[20] S.-C. Wang, Y.-W. Cheng, Y.-F. Yin et al., "Interactions of diffraction modes contributed from surface photonic crystals and nanoholes in a GaN-based light-emitting diode," *Journal of Lightwave Technology*, vol. 29, no. 24, Article ID 6065741, pp. 3772–3776, 2011.

[21] P. Vandersteegen, A. U. Nieto, C. Van Buggenhout et al., "Employing a 2D surface grating to improve light out coupling of a substrate emitting organic LED," in *Light-Emitting Diodes: Research, Manufacturing, and Applications XI*, vol. 6486 of *Proceedings of the SPIE*, pp. 64860H1–64860H8, January 2007.

[22] M. Fujita, S. Takahashi, Y. Tanaka, T. Asano, and S. Noda, "Applied physics: simultaneous inhibition and redistribution of spontaneous light emission in photonic crystals," *Science*, vol. 308, no. 5726, pp. 1296–1298, 2005.

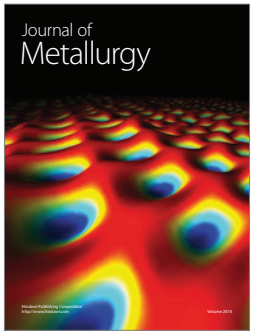

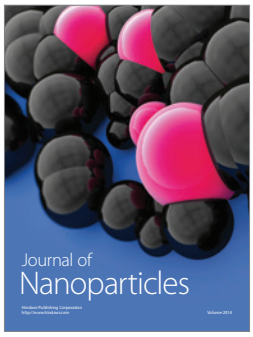

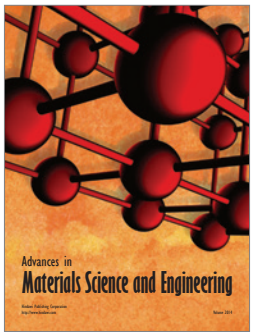

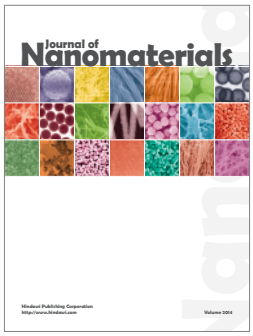

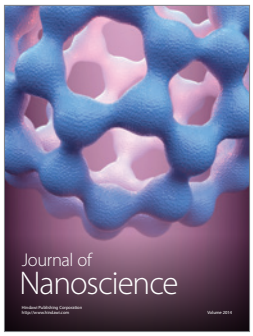

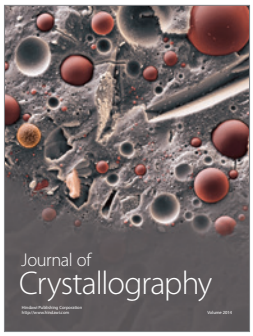

Hindawi

Submit your manuscripts at
http://www.hindawi.com